Acta Crystallographica Section F
Structural Biology and Crystallization Communications
ISSN 1744-3091

A triclinic crystal form of *Escherichia coli* 4-diphosphocytidyl-2*C*-methyl-D-erythritol kinase and reassessment of the quaternary structure

Justyna Kalinowska-Tłuścik,[a,b]‡ Linda Miallau,[c]‡ Mads Gabrielsen,[a]§ Gordon A. Leonard,[c] Sean M. McSweeney[c] and William N. Hunter[a]*

[a]Division of Biological Chemistry and Drug Discovery, College of Life Sciences, University of Dundee, Dundee DD1 5EH, Scotland, [b]Faculty of Chemistry, Jagiellonian University, ul. R. Ingardena 3, 30-060 Krakow, Poland, and [c]Macromolecular Crystallography Group, European Synchrotron Radiation Facility, BP 220, F-38043 Grenoble CEDEX 9, France

‡ These authors contributed equally to this work.
§ Current address: Division of Infection and Immunity, Faculty of Biomedical and Life Sciences, University of Glasgow, Glasgow G12 8TA, Scotland.

Correspondence e-mail: w.n.hunter@dundee.ac.uk

Received 27 October 2009
Accepted 18 December 2009

PDB Reference: 4-diphosphocytidyl-2*C*-methyl-D-erythritol kinase, 2ww4.

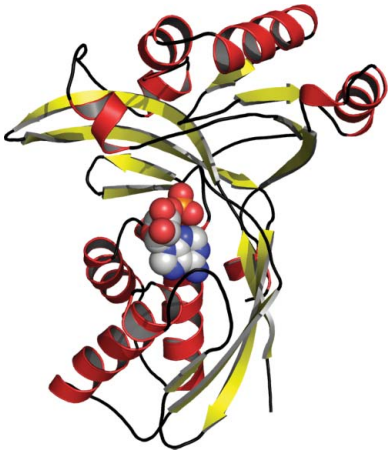

4-Diphosphocytidyl-2*C*-methyl-D-erythritol kinase (IspE; EC 2.7.1.148) contributes to the 1-deoxy-D-xylulose 5-phosphate or mevalonate-independent biosynthetic pathway that produces the isomers isopentenyl diphosphate and dimethylallyl diphosphate. These five-carbon compounds are the fundamental building blocks for the biosynthesis of isoprenoids. The mevalonate-independent pathway does not occur in humans, but is present and has been shown to be essential in many dangerous pathogens, *i.e.* *Plasmodium* species, which cause malaria, and Gram-negative bacteria. Thus, the enzymes involved in this pathway have attracted attention as potential drug targets. IspE produces 4-diphosphosphocytidyl-2*C*-methyl-D-erythritol 2-phosphate by ATP-dependent phosphorylation of 4-diphosphocytidyl-2*C*-methyl-D-erythritol. A triclinic crystal structure of the *Escherichia coli* IspE–ADP complex with two molecules in the asymmetric unit was determined at 2 Å resolution and compared with a monoclinic crystal form of a ternary complex of *E. coli* IspE also with two molecules in the asymmetric unit. The molecular packing is different in the two forms. In the asymmetric unit of the triclinic crystal form the substrate-binding sites of IspE are occluded by structural elements of the partner, suggesting that the 'triclinic dimer' is an artefact of the crystal lattice. The surface area of interaction in the triclinic form is almost double that observed in the monoclinic form, implying that the dimeric assembly in the monoclinic form may also be an artifact of crystallization.

1. Introduction

Isoprenoids are a large group of diverse compounds that are of fundamental importance to living organisms. These compounds contribute to electron transport in photosynthesis and respiration, function in photoprotection and hormone-dependent signalling and are defensive agents against pathogens (Peñuelas & Munné-Bosch, 2005; Sacchettini & Poulter, 1997). Some isoprenoids are also constituents of cell and organelle membranes and serve to protect lipids against peroxidation (Peñuelas & Munné-Bosch, 2005).

Isoprenoids are synthesized from the universal five-carbon precursors isopentenyl diphosphate and dimethylallyl diphosphate by two distinct routes. The pathways are named after their distinct intermediates. The mevalonate-biosynthetic route occurs in mammals, the cytosol and mitochondria of plants, fungi, a few eubacteria and some primitive eukaryotes such as *Trypanosoma* and *Leishmania* species (Low *et al.*, 1991; Ranganathan & Mukkada, 1995; Byres *et al.*, 2007; Sgraja *et al.*, 2007). The 1-deoxy-D-xylulose 5-phosphate (DOXP) or mevalonate-independent route is found in plant chloroplasts, cyanobacteria, eubacteria and apicomplexan parasites (Dewick, 2002; Eisenreich *et al.*, 2004; Hunter, 2007). The component enzymes of the DOXP pathway represent potential drug targets (Buetow *et al.*, 2007; Eoh *et al.*, 2007; Hunter, 2007; Crane *et al.*, 2008; Hirsch *et al.*, 2008; Sgraja *et al.*, 2008). They have no orthologues in humans and gene knockouts (*e.g.* Kobayashi *et al.*, 2003; Buetow *et al.*, 2007) have shown that these enzyme activities are essential for the survival of certain bacteria. The fact that the antimicrobial drug fosmidomycin is a potent inhibitor of DOXP reductoisomerase provides chemical validation of the pathway as a therapeutic target (Jomaa *et al.*, 1999).

Our interest centres on 4-diphosphocytidyl-2*C*-methyl-D-erythritol kinase (IspE), which catalyses the only phosphorylation stage of the

DOXP pathway: the ATP-dependent conversion of 4-diphosphocytidyl-2*C*-methyl-D-erythritol (CDP-ME) to 4-diphosphocytidyl-2*C*-methyl-D-erythritol 2-phosphate (Hunter, 2007). A high-resolution monoclinic crystal structure of the *Escherichia coli* enzyme, *Ec*IspE, has been reported and a clear picture of substrate and cofactor recognition and the mechanism of catalysis has been derived (Miallau *et al.*, 2003). In this structure two molecules constitute the asymmetric unit and we suggested that this pairing might represent a dimeric form that is observed in solution (Miallau *et al.*, 2003; Gabrielsen *et al.*, 2004).

Whilst attempting to cocrystallize *Ec*IspE with adenosine 5′-(β,γ-imino)triphosphate (AMP-PNP), an ATP analogue, and the potential inhibitor cytosine β-D-arabinofuranoside 5′-monophosphate (Ara-CMP), a different triclinic crystal form was obtained. The only ligand present is ADP. Two molecules again constitute the asymmetric unit, but the arrangement of the pair is distinct from that observed in the monoclinic crystal form. We describe the analysis of the triclinic crystal form, make comparisons with the previously determined structure and discuss the implications that the different asymmetric units have for the quaternary structure of *Ec*IspE.

2. Methods

2.1. Sample preparation, gel filtration and analytical centrifugation

The preparation of *Ec*IspE followed an established protocol (Miallau *et al.*, 2003). The molecular weight and high degree of sample purity were confirmed by sodium dodecyl sulfate–polyacrylamide gel electrophoresis and matrix-assisted laser desorption time-of-flight mass spectrometry.

Gel-filtration and analytical ultracentrifugation methods were employed to investigate the quaternary structure. Gel filtration was conducted on a Superdex 200 26/60 column calibrated with the molecular-weight standards blue dextran (>2000 kDa), thyroglobulin (669 kDa), ferritin (440 kDa), aldolase (158 kDa), conalbumin (75 kDa), ovalbumin (43 kDa), carbonic anhydrase (29.5 kDa), ribonuclease A (13.7 kDa) and aprotinin (6.5 kDa) (GE Healthcare; data not shown).

Samples for analytical ultracentrifugation were prepared at concentrations of 0.25, 0.5 and 1.0 mg ml^{-1} in 100 m*M* Tris–HCl pH 7.5, 50 m*M* NaCl, 5 m*M* dithiothreitol. Sedimentation-velocity experiments were performed (wavelength 280 nm, An50-Ti rotor, 28 000 rev min^{-1} and 293 K) using a Beckman Coulter XL-1 analytical ultracentrifuge. Samples were centrifuged simultaneously and A_{280} measurements were taken at 5 min intervals for 16 h. The resultant data were analyzed using the programs *SEDFIT* (Schuck, 2000) and *SEDNTERP* (Lebowitz *et al.*, 2002).

2.2. Crystallization and X-ray data collection

The protein (100 mg ml^{-1} in 50 m*M* Tris–HCl pH 7.7, 50 m*M* NaCl) was incubated with 3 m*M* AMP-PNP (Sigma) and 3 m*M* Ara-CMP (Sigma) on ice for 1 h to provide the stock solution for crystallization. Crystals grew in the form of fragile plates over a period of two weeks at about 293 K in hanging drops consisting of 1 µl stock solution and 1 µl reservoir solution (20% polyethylene glycol 8000, 0.2 *M* magnesium acetate, 0.1 *M* sodium cacodylate pH 6.5, 0.02 *M* dioxane).

A single crystal (of approximate dimensions 0.3 × 0.1 × 0.02 mm) was captured in a nylon loop (Hampton Research) and cooled to 100 K in a stream of nitrogen gas. Cryoprotection was achieved by soaking the crystal in mother liquor supplemented with 20%(*v*/*v*) glycerol. X-ray diffraction data were collected on beamline ID14-EH2 of the European Synchrotron Radiation Facility, Grenoble, France (λ = 0.933 Å) equipped with an ADSC Q4 CCD detector. A total of 360 images were collected with an oscillation angle of 1°. Data were integrated and intensities were scaled with *MOSFLM* (Leslie, 2006) and *SCALA* (Evans, 2006), respectively. Structure-factor amplitudes were obtained using the program *TRUNCATE* (French & Wilson, 1978).

Table 1
Crystallographic statistics for the triclinic form of IspE.

Values in parentheses are for the highest resolution shell.

Space group	*P*1
Unit-cell parameters (Å, °)	a = 49.05, b = 50.12, c = 66.04, α = 88.8, β = 69.7, γ = 65.1
Resolution range (Å)	24.9–2.0
No. of unique reflections	31885
Redundancy	1.9
Wilson *B* factor (Å^2)	16.8
Completeness (%)	94.0 (93.3)
$\langle I/\sigma(I)\rangle$	5.6 (2.9)
$R_{\rm merge}$†	6.5 (19.4)
Protein residues (monomer *A*/monomer *B*)	283/282
Water molecules	423
ADP molecules	2
Glycerol molecules	1
$R_{\rm work}$‡/$R_{\rm free}$§	19.7/26.3
R.m.s.d. from ideal values	
Bond lengths (Å)	0.011
Angles (°)	1.328
Average *B* factors (Å^2)	
Overall (monomer *A*/monomer *B*)	14.7/15.5
Side chain (monomer *A*/monomer *B*)	15.4/16.4
Main chain (monomer *A*/monomer *B*)	13.9/14.7
Waters	22.5
ADP_A	55.5
ADP_B	58.3
Glycerol	39.5
Ramachandran plot analysis (%)	
Favourable	96.2
Additionally allowed	3.4
Outliers	0.4 [Glu154 in monomers *A* and *B*]
DPI¶ (Å)	0.26

† $R_{\rm merge} = \sum_{hkl}\sum_i |I_i(hkl) - \langle I(hkl)\rangle| / \sum_{hkl}\sum_i I_i(hkl)$, where $I_i(hkl)$ is the intensity of the *i*th measurement of reflection *hkl* and $\langle I(hkl)\rangle$ is the mean value of $I_i(hkl)$ for all *i* measurements. ‡ $R_{\rm work} = \sum_{hkl} ||F_{\rm obs}| - |F_{\rm calc}|| / \sum_{hkl} |F_{\rm obs}|$, where $F_{\rm obs}$ is the observed structure-factor amplitude and $F_{\rm calc}$ is the structure-factor amplitude calculated from the model. § $R_{\rm free}$ is the same as $R_{\rm work}$ except calculated with a subset (5%) of data that were excluded from refinement calculations. ¶ The diffraction-component precision index (Cruickshank, 1999).

2.3. Structure determination and refinement

The structure of the new crystal form of *Ec*IspE was solved by molecular replacement using *AMoRe* (Navaza, 1994). Structure-factor amplitudes between 33.9 and 3.0 Å and a search model consisting of molecule *A* from the monoclinic structure of *Ec*IspE (PDB code 1oj4; Miallau *et al.*, 2003) were used. The two molecules of the asymmetric unit were positioned and then refined as a rigid body using data in the range 29.5–2.0 Å ($R_{\rm free}$ = 34.9%, figure of merit = 66.6%).

Phase information derived from the rigid-body refinement model was input into *ARP*/*wARP* (Perrakis *et al.*, 1999) for a round of automated model building. Side chains were docked to the *ARP*/*wARP* model using the *guiSIDE* module of *CCP*4*i* (Potterton *et al.*, 2003). Refinement continued with *REFMAC*5 (Murshudov *et al.*, 1999). Manual interpretation of maps was performed using *O* (Jones *et al.*, 1991) and then *Coot* (Emsley & Cowtan, 2004). Noncrystallographic symmetry restraints were used in the early stages of the refinement and were gradually released. The placement of the active-site ligands as well as water molecules and glycerol concluded the analysis. Crystallographic statistics are presented in Table 1. Analyses

of the surface areas and interactions of the distinct lattice types were made using the *PISA* service (Krissinel & Henrick, 2007) and figures were prepared with *PyMOL* (DeLano, 2002).

3. Results and discussion

3.1. Structure overview

A new triclinic crystal form of *Ec*IspE has been obtained and its structure has been determined (Table 1). The asymmetric unit consisted of two molecules labelled *A* and *B*. Superimposition of these molecules revealed only a small deviation in their overall structures, with an r.m.s.d. of 0.2 Å for an overlay of 282 C^{α} atoms. The enzyme shows the characteristic fold of the galactokinase, homoserine kinase, mevalonate kinase and phosphomevalonate kinase (GHMP) superfamily (Cheek *et al.*, 2002). The fold comprises two domains as previously described for the monoclinic structure of *Ec*IspE (Miallau *et al.*, 2003; Fig. 1).

The cofactor or ATP-binding domain is constructed from a β-sheet (β1-β4-β6-β5, with β4 antiparallel to the others) on one side of the domain and a helix bundle (α1–α4, α10) on the other. The second domain is the CDP-ME or substrate-binding domain and is created by residues 11–33 and 151–274. This domain contains two four-stranded antiparallel β-sheets (β2-β3-β7-β8 and β10-β11-β9-β12) and five helices on the surface (Fig. 1).

3.2. Comparison of crystal forms

An overlay of the two molecules in the asymmetric unit of the monoclinic crystal form (283 C^{α} atoms) gives an r.m.s.d. of 0.5 Å. The overlay of molecules *A* and *B*, using 283 and 282 C^{α} atoms, respectively, on molecules *A* and *B* of the monoclinic structure gives r.m.s.d. values in the range 0.7–0.8 Å. This indicates a high degree of structural conservation of *Ec*IspE. However, the alignment of the two molecules in the asymmetric unit of the triclinic crystal form is different from that in the monoclinic form (Fig. 2*a*). In the monoclinic structure the two molecules assemble with *C*2 symmetry, forming an extended structure (Fig. 2*b*). The surface-accessible area of the *C*2 assembly is 25 150 $Å^2$, with approximately 4% of the total surface area of a molecule or about 1000 $Å^2$ occluded from solvent (Miallau *et al.*, 2003). In the triclinic crystal form there is no obvious symmetry relationship between the molecules in the asymmetric unit and the contact area between the two molecules is approximately double that of the monoclinic form at 2080 $Å^2$, which is about 8% of the total surface area of a single molecule.

A noteworthy feature of the asymmetric unit of the triclinic crystal form is that β2, β3 and the turn that links these elements of secondary structure in molecule *A* occlude the substrate-binding pocket of molecule *B* and *vice versa*. This part of the protein occupies the site in which the α-phosphate of CDP-ME binds as seen in the monoclinic crystal form (Fig. 3). Hydrogen bonds are formed from Arg21 of one

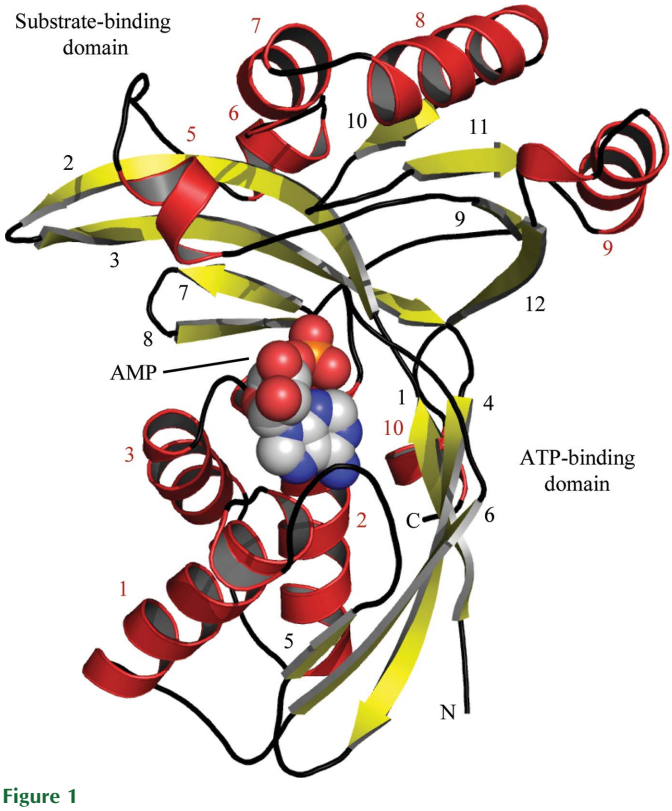

Figure 1
Ribbon representation of IspE. ADP is presented as van der Waals spheres coloured grey for C, red for O, orange for P and blue for N. The N- and C-termini are labelled. β-Strands are shown in yellow and α-helices are shown in red; they are numbered in black and red, respectively.

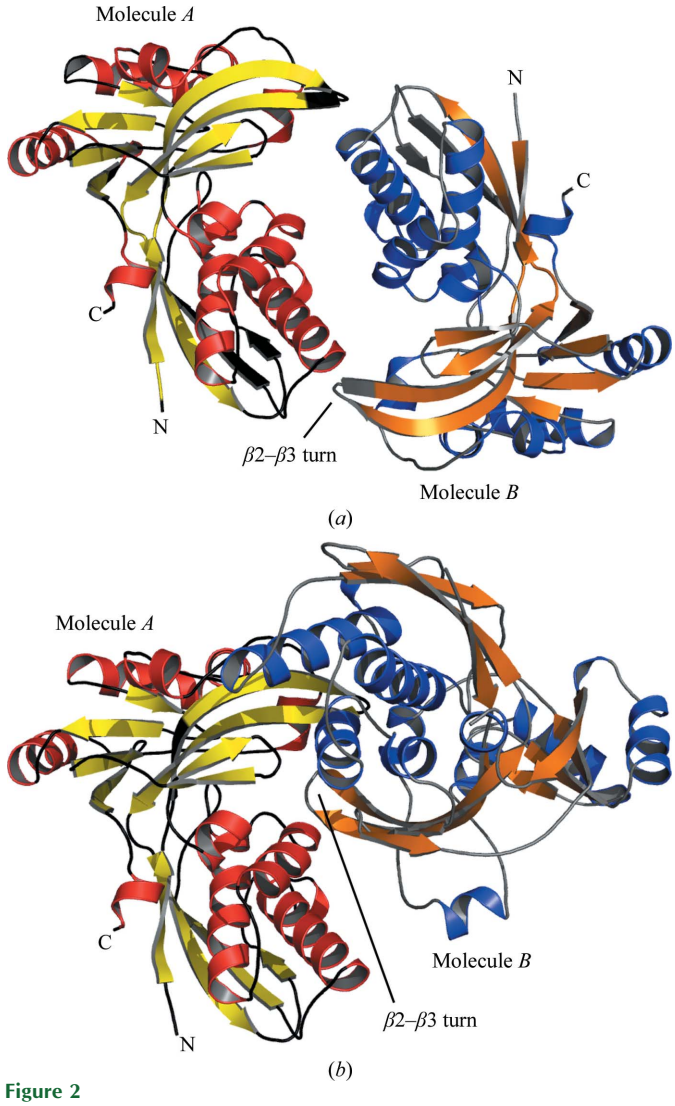

Figure 2
Comparison of the distinct asymmetric units observed for *E. coli* IspE. (*a*) The monoclinic crystal form (Miallau *et al.*, 2003; PDB code 1oj4). (*b*) The triclinic form of the enzyme. For each structure, molecule *A* is shown in the same orientation and the position of the β2–β3 turn of molecule *B* is marked.

molecule to Tyr25 OH and the main-chain carbonyl of Leu136 of the other molecule (data not shown) in both cases. Tyr25 is important for interaction of *Ec*IspE with the substrate since the hydroxyl group donates a hydrogen bond to the α-phosphate and the side chain forms van der Waals interactions with the pyrimidine moiety of CDP-ME (Miallau *et al.*, 2003). In this assembly the enzyme would be unable to bind its substrate and we judge it likely that this alignment of the two *Ec*IspE molecules is an artefact of crystallization. Given then that this potential artefact produced a protein–protein interface surface area larger than that observed in the monoclinic crystal form we thought it necessary to investigate the quaternary structure in more detail.

We previously showed by gel filtration and analytical ultracentrifugation that *Aquifex aeolicus* IspE is monomeric in solution (Sgraja *et al.*, 2008). For *Ec*IspE the elution profile obtained by gel filtration was in good agreement with the analytical ultracentrifugation data and indicated that *Ec*IspE is predominantly a monomer (with a mass of approximately 33 kDa) in solution with some dimeric species also present; we estimate the ratio to be approximately 4:1 (data not shown). We analysed the crystal packing of both crystal forms in detail to investigate whether there could be another combination of molecules with a sufficiently large surface area and conserved interactions to suggest a physiologically relevant dimer. We could find no such pair.

3.3. Ligand binding

Although Ara-CMP was present in the crystallization mixture and was expected to occupy the substrate-binding site, we did not observe any electron density corresponding to this potential *Ec*IspE inhibitor. The electron density in the two ATP-binding pockets was interpreted as ADP (Fig. 4). Since AMP-PNP was initially added to the enzyme, we assume that either hydrolysis has occurred or there is disorder of the polyanionic tail in this crystal form.

Superimposition of the *Ec*IspE–AMP-PNP complex determined in the monoclinic crystal form on the triclinic crystal form molecules indicates a good agreement in the location of the adenine in the binding pocket and the conservation of hydrogen-bonding and van der Waals interactions. In particular, the amine N atom of adenine donates two hydrogen bonds to the side-chain carbonyls of Asn65 and Asn110 and the adenine N7 accepts a hydrogen bond donated by the amide of Leu66 (data not shown). The ribose and phosphate moieties of ADP adopt slightly different positions relative to the corresponding parts of AMP-PNP. The ADP phosphate groups are both positioned close to the AMP-PNP β-phosphate (data not shown).

4. Conclusions

Two crystal structures of *Ec*IspE have been determined, each with two molecules in the asymmetric unit. The arrangement of the molecules in the asymmetric unit and the interactions in the crystal lattice are distinctive for each crystal form. Gel-filtration and analytical ultracentrifugation experiments indicated that the predominant form of *Ec*IspE in solution was a monomer and that there was a small amount of dimer present. This is consistent with the observation that the active site of *Ec*IspE is wholly formed by a single polypeptide chain with no apparent reliance on a partner subunit for catalysis and with the previous work on *A. aeolicus* IspE which indicates that the enzyme is a monomer (Sgraja *et al.*, 2008). It is noteworthy that the asymmetric unit pairing observed in the triclinic form actually blocks the substrate-binding site of both molecules. We take this to suggest that crystal-packing effects determine the IspE pairing observed in the triclinic structure. There is evidence that IspE interacts with and forms higher order complexes with enzymes that are adjacent in the DOXP pathway, namely IspD and IspF (Gabrielsen *et al.*, 2004). The formation of a dimer may facilitate this process, serving to satisfy the stoichiometry necessary for the assembly of a large three-enzyme

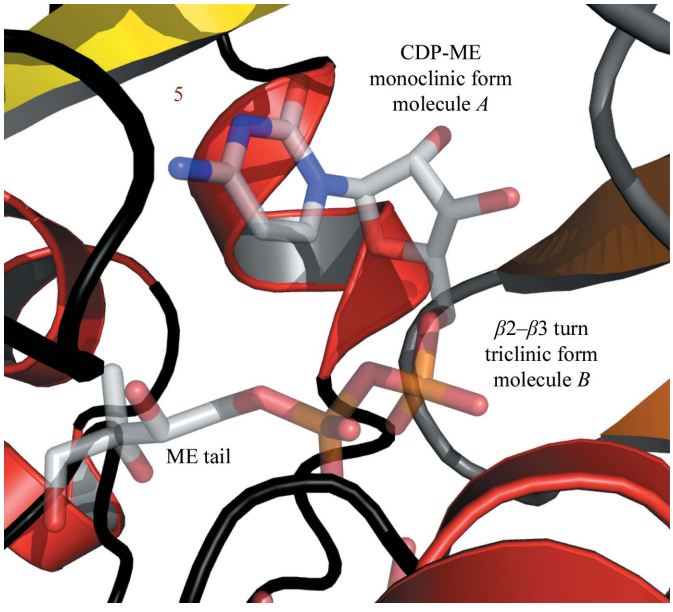

Figure 3
One *Ec*IspE active site in the triclinic structure is occluded by the asymmetric unit partner. The substrate-binding pocket of the triclinic form molecule *A* is shown together with the $\beta2$–$\beta3$ turn of molecule *B*. CDP-ME from molecule *A* of the monoclinic structure, after least-squares superposition of the *A* molecules, is shown as semi-transparent sticks and with the same atomic colouring scheme as employed in Fig. 1.

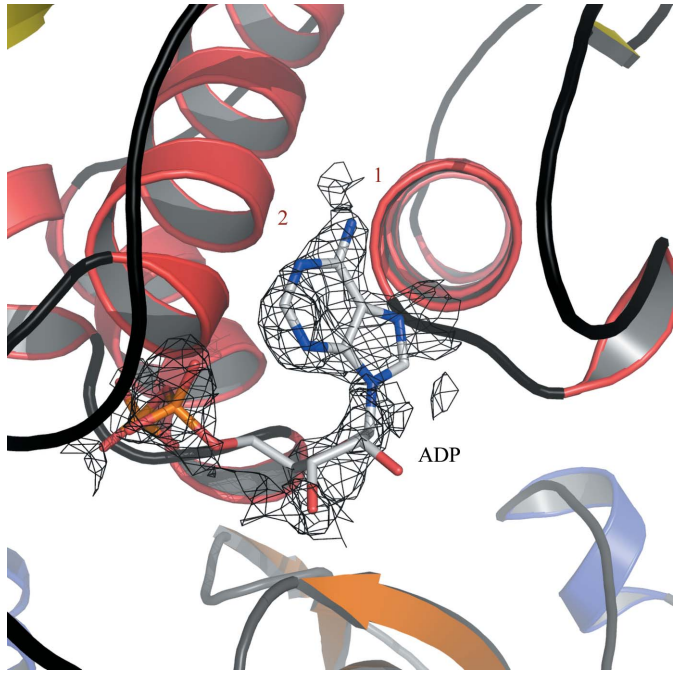

Figure 4
ADP in the cofactor-binding pocket. The OMIT $F_o - F_c$ difference density map is shown as black chicken wire and contoured at 1.5σ. $\alpha1$ and $\alpha2$ are labelled in red.

complex to carry out a metabolic function. Such an assembly co-localizes different enzyme activities and may enhance the efficiency of isoprenoid-precursor biosynthesis. However, the surface area between the two molecules in the triclinic form asymmetric unit is significantly larger than observed in the monoclinic form. This suggests that we should be cautious about whether the dimer observed in the monoclinic form is representative of the dimeric species observed in solution.

This work was supported by awards from the BBSRC (Structural Proteomics of Rational Targets; BBS/B/14434), The Wellcome Trust (grant Nos. 082596 and 083481) and ESRF Grenoble.

References

Buetow, L., Brown, A. C., Parish, T. & Hunter, W. N. (2007). *BMC Struct. Biol.* **7**, 68.

Byres, E., Alphey, M. S., Smith, T. K. & Hunter, W. N. (2007). *J. Mol. Biol.* **371**, 540–553.

Cheek, S., Zhang, H. & Grishin, N. V. (2002). *J. Mol. Biol.* **320**, 855–881.

Crane, C. M., Hirsch, A. K., Alphey, M. S., Sgraja, T., Lauw, S., Illarionova, V., Rohdich, F., Eisenreich, W., Hunter, W. N., Bacher, A. & Diederich, F. (2008). *Chem. Med. Chem.* **3**, 91–101.

Cruickshank, D. W. J. (1999). *Acta Cryst.* D**55**, 583–601.

DeLano, W. L. (2002). *PyMOL Molecular Viewer.* http://www.pymol.org.

Dewick, P. M. (2002). *Medicinal Natural Products: A Biosynthetic Approach*, 2nd ed., pp. 167–289. Chichester: John Wiley & Sons.

Eisenreich, W., Bacher, A., Arigoni, D. & Rohdich, F. (2004). *Cell. Mol. Life Sci.* **61**, 1401–1426.

Emsley, P. & Cowtan, K. (2004). *Acta Cryst.* D**60**, 2126–2132.

Eoh, H., Brown, A. C., Buetow, L., Hunter, W. N., Parish, T., Kaur, D., Brennan, P. J. & Crick, D. C. (2007). *J. Bacteriol.* **189**, 8922–8927.

Evans, P. (2006). *Acta Cryst.* D**62**, 72–82.

French, S. & Wilson, K. (1978). *Acta Cryst.* A**34**, 517–525.

Gabrielsen, M., Bond, C. S., Hallyburton, I., Hecht, S., Bacher, A., Eisenreich, W., Rohdich, F. & Hunter, W. N. (2004). *J. Biol. Chem.* **279**, 52753–52761.

Hirsch, A. K. H., Alphey, M. S., Lauw, S., Seet, M., Barandun, L., Eisenreich, W., Rohdich, F., Hunter, W. N., Bacher, A. & Diederich, F. (2008). *Org. Biomol. Chem.* **6**, 2719–2730.

Hunter, W. N. (2007). *J. Biol. Chem.* **282**, 21573–21577.

Jomaa, H., Wiesner, J., Sanderbrand, S., Altincicek, B., Weidemeyer, C., Hintz, M., Türbachova, I., Eberl, M., Zeidler, J., Lichtenthaler, H. K., Soldati, D. & Beck, E. (1999). *Science*, **285**, 1573–1576.

Jones, T. A., Zou, J.-Y., Cowan, S. W. & Kjeldgaard, M. (1991). *Acta Cryst.* A**47**, 110–119.

Krissinel, E. & Henrick, K. (2007). *J. Mol. Biol.* **372**, 774–797.

Kobayashi, K. *et al.* (2003). *Proc. Natl Acad. Sci. USA*, **100**, 4678–4683.

Lebowitz, J., Lewis, M. S. & Schuck, P. (2002). *Protein Sci.* **11**, 2067–2079.

Leslie, A. G. W. (2006). *Acta Cryst.* D**62**, 48–57.

Low, P., Dallner, G., Mayor, S., Cohen, S., Chait, B. T. & Menon, A. K. (1991). *J. Biol. Chem.* **266**, 19250–19257.

Miallau, L., Alphey, M. S., Kemp, L. E., Leonard, G. A., McSweeney, S. M., Hecht, S., Bacher, A., Eisenreich, W., Rohdich, F. & Hunter, W. N. (2003). *Proc. Natl Acad. Sci. USA*, **100**, 9173–9178.

Murshudov, G. N., Vagin, A. A., Lebedev, A., Wilson, K. S. & Dodson, E. J. (1999). *Acta Cryst.* D**55**, 247–255.

Navaza, J. (1994). *Acta Cryst.* A**50**, 157–163.

Peñuelas, J. & Munné-Bosch, S. (2005). *Trends Plant Sci.* **10**, 166–169.

Perrakis, A., Morris, R. & Lamzin, V. S. (1999). *Nature Struct. Biol.* **6**, 458–463.

Potterton, E., Briggs, P., Turkenburg, M. & Dodson, E. (2003). *Acta Cryst.* D**59**, 1131–1137.

Ranganathan, G. & Mukkada, A. J. (1995). *Int. J. Parasitol.* **25**, 279–284.

Sacchettini, J. C. & Poulter, C. D. (1997). *Science*, **277**, 1788–1789.

Schuck, P. (2000). *Biophys. J.* **78**, 1606–1619.

Sgraja, T., Alphey, M. S., Ghilagaber, S., Marquez, R., Robertson, M. N., Hemmings, J. L., Lauw, S., Rohdich, F., Bacher, A., Eisenreich, W., Illarionova, V. & Hunter, W. N. (2008). *FEBS J.* **275**, 2779–2794.

Sgraja, T., Smith, T. K. & Hunter, W. N. (2007). *BMC Struct. Biol.* **30**, 20.